

## HIGH TEMPERATURE OXIDATION OF A ZIRCONIUM BASE ALLOY IN STEAM

KWANGHEON PARK<sup>1)</sup>, TAEGEUN YOO<sup>1)</sup>, SUNGKWON KIM<sup>1)</sup>  
HYUN-GIL KIM<sup>2)</sup>, YONGHWAN JEONG<sup>2)</sup>, KYUTAE KIM<sup>3)</sup>

<sup>1)</sup>Kyunghee University, South Korea

<sup>2)</sup>Korea Atomic Energy Research Institute

<sup>3)</sup>KEPCO Nuclear Fuel Company, South Korea

### Abstract

High temperature steam oxidation behaviors of a Zirconium alloy, Zr-1%Nb alloy was examined for the comparison to those of Zircaloy-4 (Zry-4). Testing temperatures were 700 – 1200°C. At atmospheric steam pressure, oxidation kinetics of Zr-1%Nb alloy follows parabolic-rate law, instead of cubic-rate as was observed in Zry-4 below 900 °C. The oxidation rate of Zr-1%Nb alloy is slightly lower than that of Zry-4. A double layer autoclave, that can make high steam pressures up to 150bar and temperatures up to 900 °C, was used to get the steam pressure effects on high temperature oxidation. Zry-4 was very sensitive to the steam pressure, and the oxidation rate increases exponentially with applied steam pressure. Zr-1%Nb alloy was less sensitive to the high-pressure steam. The enhancement parameter is about 3 to 13 times lower than that of Zry-4. The stability of tetragonal phase in the Zr-1%Nb alloy comparing Zry-4 seems to make the difference in oxidation kinetics.

### 1. INTRODUCTION

Zr-base alloys are used as cladding materials for nuclear fuel in light and heavy water reactors. Zircaloy-4 (Zry-4) has been used satisfactorily as a cladding material in pressurized water reactors. Nowadays, light water reactors tend to extend their fuel cycle length with high burn-up of nuclear fuel to get the improved economy. Zry-4 may not satisfy the required safety margin for the high burn-up fuel, and more corrosion-resistant Zr-base cladding materials are being developed. One direction for the development of new Zr-base alloys is addition of Nb in alloying elements.

At high temperatures, the exothermic reaction of Zr-base alloys with steam is always a concern for the safety of nuclear power plants during accidents like a loss-of-coolant accident. The Nuclear Regulatory Commission still uses the same criteria, which are applied to conventional Sn-added Zr claddings, for the safety analysis of newly developed Nb-added Zr base alloys. So, it is needed to check the difference in the kinetics of high-temperature oxidation in between Nb-added and Sn-added Zr alloys. In the present paper, we compare the characteristics of Sn-added Zr-alloy (Zry-4) and those of Nb-added alloy (Zr-1%Nb alloy), especially at high temperature oxidation.

## 2. EXPERIMENTALS

We selected two types of specimens, i.e., Zry-4 as a Sn-added alloy and Zr-1%Nb alloy as a Nb-added alloy in the experiments. Zry-4 tubes are the commercial tubes of Westinghouse, and used in the as-supply state. The tubes were cut to specimens of the height of about 15mm. Each specimen was degreased and pickled in aqueous HF/HNO<sub>3</sub> solution, then cleansed in hot and cold water. The chemical composition of each type of specimens is shown in Table 1. The main alloying elements of Zry-4 are Sn, Fe and Cr, while those of Zr-1%Nb alloy are Nb, Sn, and Fe.

Table 1. Chemical composition of Zry-4 and Zr-1%Nb alloy.

Alloy	Nb	Sn	Fe	Cr	O	C
Zry-4	n.a.	1.1-1.5	0.2-0.24	0.06-0.14	1090ppm	120ppm
Zr-1%Nb alloy	1.01	1.06	0.1	60ppm	1200ppm	60ppm

(Units: w/o if not specified)

High temperature oxidation tests were done under 1 atm steam in a vertical heater, where a specimen is hung by a Pt-wire. When the goal temperature is obtained and the steam flow through the alumina tube inside heater becomes stabilized, the specimen is inserted into the center of the tube and pulled out of the tube after the desired oxidation is reached. The temperature range is in between 700 and 1200°C. The steam flow rate is about 10g/min. After oxidation test, the specimen is molded, grounded and polished for the optical microscopic observation. For the micro-structural evaluation, sometimes the polished section was wipe-polished by etchant. The thickness of oxide and that of alpha-layer are determined by the photos from optical microscope.

The steam-pressure dependency of Zr-alloys on the oxidation at high temperatures was also observed. The dependency was obtained by an experimental setup that consists of two vessels and two resistance heaters (Fig.1). The outer vessel is used for maintaining high-pressure steam during the experiment. The vessel is heated up to 400°C, and the steam pressure is controlled by the amount of water inside the vessel up to 150bar steam. Once the

steam pressure is stabilized, the resistance heater surrounding the specimen inside the inner vessel is on. The specimen is heated up to the set-up temperature (700-900 °C) rapidly by the resistance heater. The heat up rate of the specimen is about 3 °C/sec, and oxidation time was set to 1500sec.

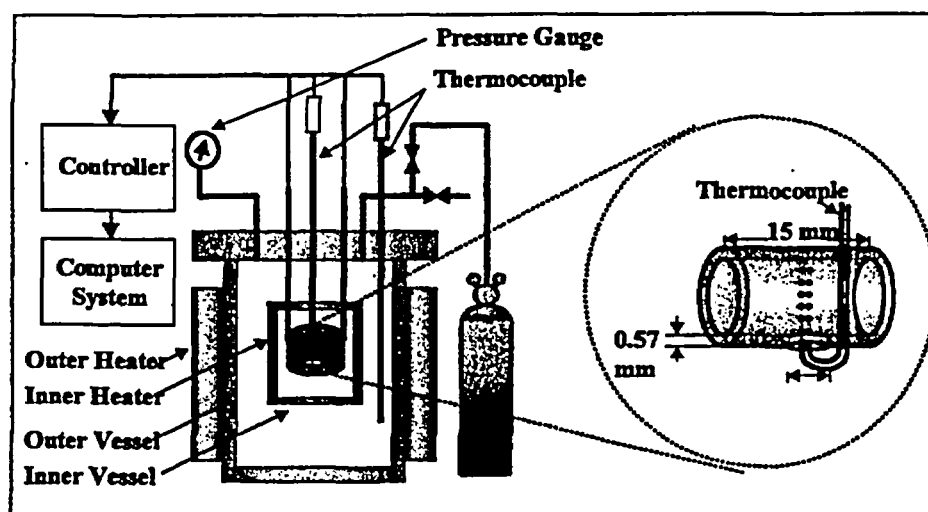


Fig. 1. Experimental setup for high-pressure steam oxidation

After oxidation, the specimen is cooled down with a rate of about 1.5 °C/sec. The specimen used in high-pressure steam experiments has a drilled hole (about 3mm dia.). The specimen is hung and contacted by a thermocouple through this hole (Fig.1). The oxide thickness is measured from the observation by the optical microscope or scanning electron microscope (SEM). Oxide surface and morphology were also examined.

### 3. RESULTS AND DISCUSSION

The oxidation test at 1 atm steam is shown in Fig.2. The symbols (solid lines) indicate the weight gains of Zr-1%Nb alloy specimens with time and the dashed lines are those of Zry-4. Below 900°C, transition points are observed in both alloys. Parabolic rate law is always applicable before transition in Zr-1%Nb alloy. The weight gain of Zr-1%Nb alloy at atmospheric steam can be formulated by the following equations.

Before transition, the weight gain ( $\Delta W$ ) becomes;

$$\Delta W = K_p \sqrt{t}$$

where  $K_p = 7.139 \times 10^4 \exp\left(\frac{-10,665.7}{T(K)}\right)$  and  $\Delta W : \text{mg/dm}^2, t : \text{sec.}$

After the transition point (below 900°C), the weight gain becomes;

$$\Delta W = Wt + K_1(t - t_T)$$

$$\text{where } Wt = 1.286 \times 10^7 \exp\left(\frac{-11,964}{T(K)}\right)$$

$$K_1 = 1.51 \times 10^2 \exp\left(\frac{-8,303}{T(K)}\right)$$

$$t_T = 3.23 \times 10^4 \exp\left(\frac{-2,579}{T(K)}\right)$$

The above kinetic equation is denoted as solid lines in Fig.2. The oxidation kinetics of Zr-1%Nb alloy is somewhat different from those of Zry-4. The kinetic constant,  $K_p$  is compared with the values of other works (Table 2) [1-5]. Generally, activation energy of the kinetic constant in oxidation of Zr-1%Nb alloy is very close to that of Zry-4, however, the kinetic constant is slightly less. At the temperatures of monoclinic-oxide stable region (below 1000°C), a cubic rate law is noticeable in Zry-4 before transition. In Zr-1%Nb alloy, parabolic rate is always observed. This cubic to parabolic rate change in the monoclinic oxide region seems one of the characteristic changes by the addition of Nb. Sn is a mostly contained alloying element in Zr-1%Nb alloy, the contribution to kinetics is much less than that of Nb. The oxidation amount of Zr-1%Nb alloy below 1000°C is comparable or larger than that of Zry-4. At the temperatures above 1000°C, the oxidation rate of Zr-1%Nb alloy is lower than Zry-4.

Table 2. Parabolic rate constants in Zr alloys.  $K_p = A \exp(Q/RT)$ .

Temp. range(°C)	A (mg/dm <sup>2</sup> )	Q (kcal)	Materials	Reference
1000 - 1850	$20.2 \times 10^4$	22.75	Zr	1
1050 - 1580	$1.91 \times 10^4$	16.7	Zry-2, Zry-4	2
1000 - 1300	$7.24 \times 10^4$	20.83	Zry-4	3
1050 - 1500	$6.02 \times 10^4$	19.97	Zry-4	4
700 - 1100	$4.873 \times 10^4$	20.4	Zr-1w/oNb	5
700 - 1200	$7.139 \times 10^4$	21.2	Zr-1%Nb alloy	This work

Oxide thickness of Zr-1%Nb alloy and that of Zry-4 is compared in Fig.3. The oxide layer growth of both alloys looks very proportional to their weight gain.

Above 860°C, the cross-sectional view of each specimen shows the well-known three-layer structure - oxide, oxygen-stabilized  $\alpha$ -layer and prior  $\beta$ -layer (or,  $\alpha'$ -layer). Fig.4 displays the

3-layer structure in the specimens of Zry-4 and Zr-1%Nb alloy oxidized at 1200 °C for 5 minutes. The distinction between  $\alpha$ -stabilized  $\alpha$ - and prior  $\beta$ - layers in Zry-4 is noticeable, while the distinction is somewhat not clear in Zr-1%Nb alloy. Some microcracks are observable between  $\alpha$ - and prior  $\beta$ -layers in Zr-1%Nb alloy. The  $\alpha$ -layer of Zr-1%Nb alloy looks thinner than that of Zry-4.

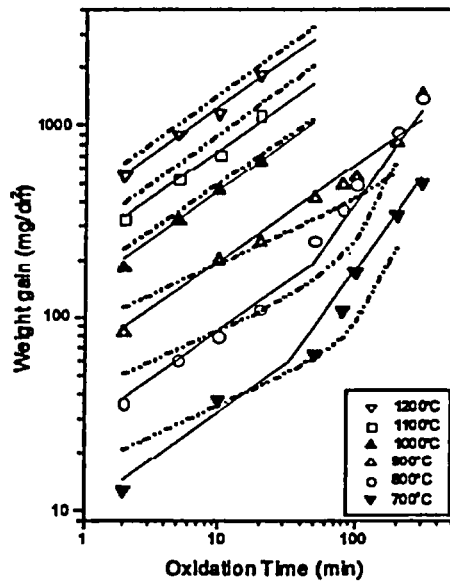


Fig.2. Weight gain of Zr-1%Nb alloy in 1atm Steam. (dashed lines:Zry-4)

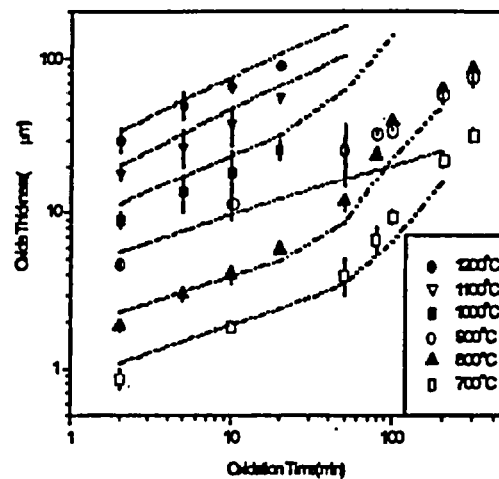


Fig.3. Oxide thickness of Zr-1%Nb alloy (dashed lines: Zry-4)

The oxide layers of both alloys have columnar structures. The prior  $\beta$ -layer in Zr-1%Nb alloy is shown to be finer Widmannstatten structure than that in Zry-4. However, the discontinuous lines between  $\alpha$ - and  $\beta$ - grains are not clearly noticeable in Zr-1%Nb alloy specimens. We set the thickness of  $\alpha$ -layer as the length between oxide boundary and fine microcracks. Fig.5 is the comparison graph of the thickness of  $\alpha$ -layers in Zry-4 and Zr-1%Nb alloy. As shown in Fig.4, the  $\alpha$ -layer growth rate of Zr-1%Nb alloy specimens (symbols) is lower than that of Zry-4 (dashed lines). And, the kinetics is also different. In Zry-4,  $\alpha$ -layer growth follows the time dependency of the power of  $\sim 0.5$  ( $t^{0.5}$ ). However, the slope of the time dependence is quite different in Zr-1%Nb alloy, usually with the power of  $0.2 \sim 0.35$  ( $t^{0.2-0.35}$ ).

The radial hardness profile of the specimens was also measured. Fig.6 and 7 show the

results of hardness measurements of Zry-4 and Zr-1%Nb alloy specimens, respectively. The oxide hardness was not included in the figures. The hardness decreases sharply in  $\alpha$ -layers, then the value decreases slowly or stays constant in prior  $\beta$ -region. The hardness is known to depend on the oxygen content in metal, and  $\alpha$ -layer has higher hardness number than  $\beta$ -layer. The oxidation temperature dependency of hardness in prior  $\beta$ -layers in Zr-1%Nb alloy is quite different from that of Zry-4. Hardness values increase with the oxidation temperature, probably due to the higher oxygen content in the matrix during oxidation at higher temperatures. Hardness of metal matrix ( $\beta$ -layer) increases more strongly with oxidation temperature in Zr-1%Nb alloy than in Zry-4.

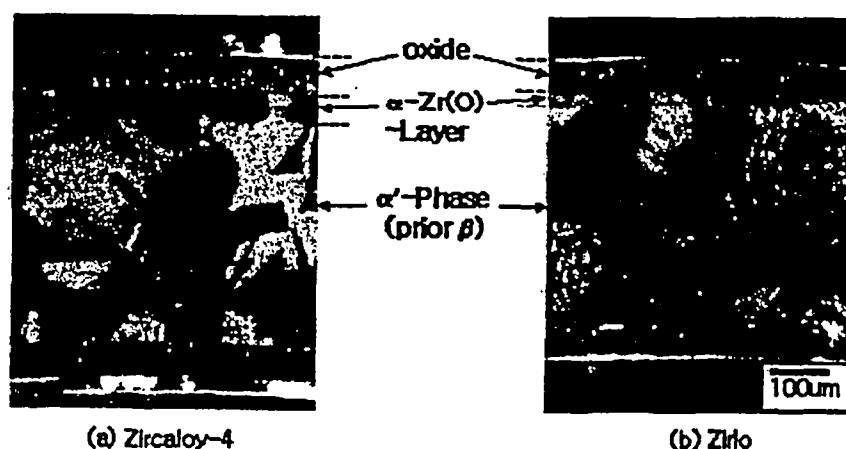


Fig.4. Cross-sectional view of Zry-4(a) and Zr-1%Nb alloy(b) specimens.

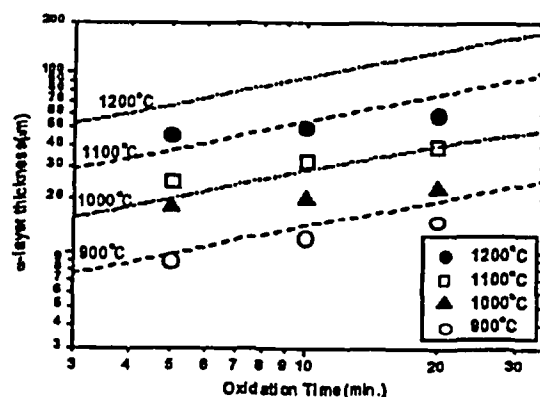


Fig.5.  $\alpha$ -layer growth with time. Symbols: Zr-1%Nb alloy, dash lines: Zry-4.

The increase of hardness in metal matrix is important from the viewpoint of severe accidents, since the hardness increase means the reduction of ductility in Zr-1%Nb alloy. Bonmert, et al., checked the safety margin of Zr-1%Nb alloy at severe accident conditions [5]. NRC requires the calculated equivalent cladding reacted (ECR) must not exceed 17% of the cladding wall thickness during accidents. Ring compression test indicates the ductility at 5% of ECR in Zr-1w/oNb alloy is already lower than that of 18% ECR in Zry-4 cladding [5].

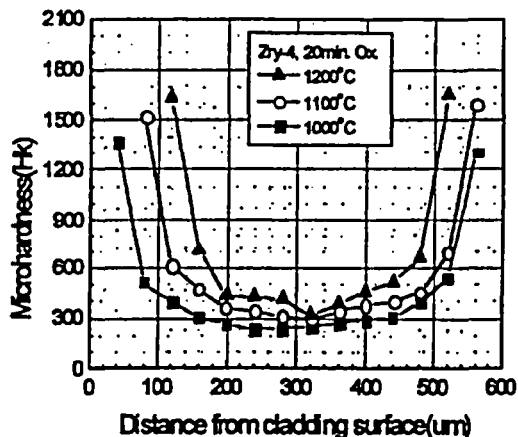


Fig. 6. Hardness of Zry-4 after 20 minute oxidation

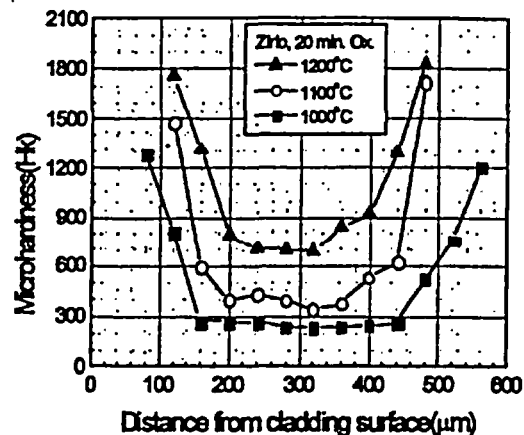


Fig.7. Hardness of Zr-1%Nb alloy after 20 minute oxidation.

The reason for the hardness increase seems from the increase of oxygen content in metal matrix. The higher hardness of Zr-1%Nb alloy ( $\beta$ -region) means that Zr-1%Nb alloy has higher oxygen content in metal matrix than Zry-4 does. Hence, it is highly probable that Zr-1%Nb alloy has the higher equilibrium oxygen concentration in  $\beta$ -phase at the phase boundary than Zry-4. Nb, a bcc structural element, tends to stabilize  $\beta$ -phase that is bcc. So, it may be reasonable to think that  $\beta$ -phase contains more oxygen if Nb is added.

Pawel[6] and Brown et al. [7] measured the diffusion coefficient of oxygen in  $\beta$ -phase by fitting the calculation of diffusion equation with metallographic data. The characteristic time of diffusion in the  $\beta$ -layer ( $t = l^2 / D$ ,  $l = 0.035\text{cm}$ ) can be approximately calculated. Table 3 indicates the diffusion coefficient and the characteristic time at each temperature for the specimen used. Comparing the oxidation time (20 min.) to the characteristic time, the oxygen concentration in  $\beta$ -region is nearly saturated at least in the specimen oxidized at 1200°C. Hence, the amount of oxygen concentration difference, that makes the hardness difference in metal layers, should be the difference in the equilibrium oxygen concentration of  $\beta$ -phase between Zr-1%Nb alloy and Zry-4.

Table 3. Diffusion coefficient of oxygen in  $\beta$ -phase and characteristic time.  
Specimen half-length is about 0.035cm.

Temp. (°C)	Diff. coeff. (cm <sup>2</sup> /sec) [6,7]	Char. time (min.)
1200	$1.5 \sim 1.7 \times 10^{-6}$	12 ~ 14
1100	$7.1 \sim 8.6 \times 10^{-7}$	24 ~ 29
1000	$3.0 \sim 3.8 \times 10^{-7}$	53 ~ 67

The results of oxidation enhancement by high-pressure steam are shown in Fig.8 and 9. The oxidation time is set 1500sec. Both Zry-4 and Zr-1%Nb alloy clearly show the enhancement of oxidation under high steam pressure. And, the oxidation enhancement depends exponentially on the steam pressure. The dependency of Zr-1%Nb alloy is much smaller than that of Zry-4 (Fig.9). The enhancement can be expressed in the following equation,

$$d(P) = d(1) \cdot \exp(H \cdot P)$$

where,  $d(P)$ ,  $d(1)$ : oxide thickness at P bar and 1 bar steam, respectively.

$H$ : enhancement parameter (bar<sup>-1</sup>),  $P$ :bar,

Table 4 is the fitting results of the enhancement parameter, H using above equation. The value of H in Zry-4 is about 4~13 times higher than that in Zr-1%Nb alloy.

Pawel has measured the oxide thickness at 900 and 1100°C in high pressure steam[8]. At 1100°C, there was no difference in oxide layer growth rate with steam pressure, while the increase of oxidation rate was evident at 900°C. One big difference between steam oxidation at 900 and at 1100°C is the stability of tetragonal phase. At 900°C, tetragonal oxide is thermodynamically unstable and becomes monoclinic phase, once the restrictive conditions (compressive stress, small grains) are removed. However, tetragonal phase is stable throughout the oxidation at 1100°C regardless of steam pressure. Based on this observation, it can be postulated that the pressure effect on the oxidation rate is originated from the stability of tetragonal phase (or tetragonal to monoclinic phase transformation).

Loss of tetragonal phase during oxidation induces two detrimental effects: non-protective monoclinic phase formation and tension appearance at the oxide surface. Especially, sudden loss of tetragonal phase during oxidation induces the volume expansion (about 3%) at monoclinic/tetragonal interface, resulting in huge tension at the oxide surface. And, high-pressure steam destabilizes the tetragonal phases by reducing the surface energy of monoclinic embryos. Loss of tetragonal phase makes non-protective monoclinic oxides and crack formation on the oxide surface, resulting in oxidation enhancement.



Based on H values, it can be concluded that the tetragonal phase formed on Zr-1%Nb alloy cladding is more stable than that on Zry-4.

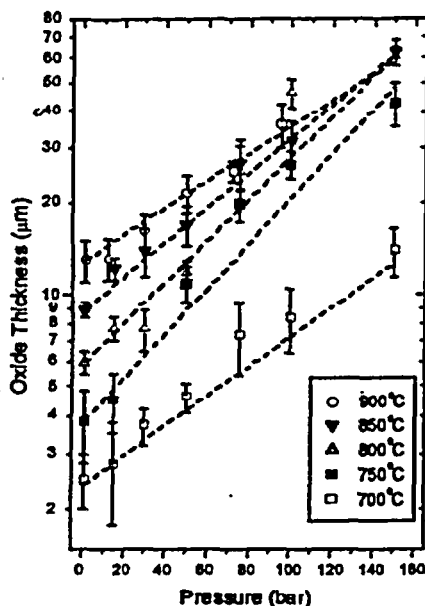


Fig.8. Steam pressure effects on the oxidation of Zry-4.

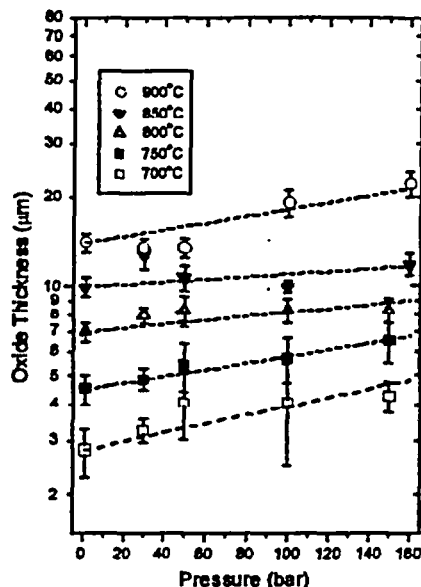


Fig.9. Steam pressure effects on the oxidation of Zr-1%Nb alloy.

Table 4. Value of H in Zry-4 and Zr-1%Nb alloy. H: bar<sup>-1</sup>

Temp(°C)	900	850	800	750	700
Zry-4	$1.01 \times 10^{-2}$	$1.29 \times 10^{-2}$	$1.55 \times 10^{-2}$	$1.69 \times 10^{-2}$	$1.11 \times 10^{-2}$
Zr-1%Nb alloy	$2.59 \times 10^{-3}$	$1.00 \times 10^{-3}$	$1.55 \times 10^{-3}$	$2.53 \times 10^{-3}$	$3.40 \times 10^{-3}$

#### 4. CONCLUSION

High temperature steam oxidation behaviors of Zr-1%Nb alloy and Zry-4 were compared. Oxidation tests with destructive analyses were done to get the kinetics, and testing temperatures were 700 – 1200°C. As-received tube specimens were cut 1.5cm high, etching finished, and used for the test. Oxidation kinetics of Zr-1%Nb alloy at atmospheric steam pressure, follows parabolic-rate law, instead of cubic-rate as was observed in Zry-4 below 900 °C. The oxidation rate of the Zr-alloy is comparable to that of Zry-4 below 900 °C , however, is slightly lower than Zry-4 above 1000 °C.

Steam pressure effects on high temperature oxidation of both Zr-1%Nb alloy and Zry-4 were measured by a double layer autoclave, which can make high steam pressures up to 150bar and temperatures up to 900 °C. Oxidation time was set to 1500sec. Zry-4 was very sensitive to the steam pressure, and the oxidation rate increases exponentially with applied steam pressure. Contrary to Zry-4, the Zr-alloy was less sensitive to the high-pressure steam. The exponential dependency (i.e., enhancement parameter) of Zr-1%Nb alloy is about 3~13 times lower than that of Zry-4. High-pressure steam destabilizes tetragonal oxides, seemingly by reducing the surface energy between monoclinic and tetragonal phases. Loss of tetragonal phase makes non-protective monoclinic oxides and crack formation on the oxide surface, resulting in oxidation enhancement. The stability of tetragonal phase in the Zr-1%Nb alloy comparing Zry-4 seems to make the difference in oxidation kinetics.

#### ACKNOWLEDGEMENT

This work is supported from the KEPCO Nuclear Fuel Co., LTD, under the national program for mid- and long term research and development of nuclear energy by MOST.

#### REFERENCES

1. L.Baker and L.C.Just, ANL-6248 (1962)
2. V.F.Urbanić and T.R.Heidrick, J. Nucl. Mater., 75 (1978) 251
3. S.Leistikow and G.Schanz, Nucl. Eng. Design, 103 (1987) 65
4. R.E.Pawel, J.V.Cathcart and R.A.McKee, J. Electrochem.: Sci. & Tech., 126 (1979) 1105
5. J.Bohmert, M.Dietrich and J.Linek, Nucl. Eng. Design, 147 (1993) 53
6. R.E.Pawel, J. Electrochem. Soc., 126 (1979) 1111
7. A.F.Brown, M.O.Tucker, T.Healey and C.J.Simpson, J. Nucl. Mater., 105 (1982) 93
8. R.E.Pawel, J.V.Cathcart and J.J.Campbell, J. Nucl. Mater., 82 (1979) 129